Supplementary Information

Morphology – composition correlations in carbon nanotubes synthesised with nitrogen and phosphorus containing precursors

Rebecca J. Nicholls,[a] Zabeada Aslam,[a,†] Michael C. Sarahan,[b,‡] Ana M. Sanchez,[c] Frank Dillon,[a] Antal A. Koós,[a,§] Peter D. Nellist[a,b] and Nicole Grobert[a]

[a] Department of Materials, University of Oxford, Oxford OX1 3PH, UK

[b] SuperSTEM Laboratory, STFC Daresbury, Warrington WA4 4AD, UK

[c] Department of Physics, University of Warwick, Coventry CV4 7AL, UK.

† present address: Institute for Materials Research, School of Chemical and Process Engineering (SCAPE), University of Leeds, Leeds LS2 9JT, UK

‡ present address: Nion Co., 1102 8th Street, Kirkland, WA 98033, USA

§ present address: Institute for Technical Physics and Materials Research, Hungarian Academy of Sciences, Hungary

Amorphous material on the inner-wall of the nanotube

Amorphous material is shown in the inner channel of the nanotube in Figures 1d, a larger image of this nanotube is shown in Figures S1.

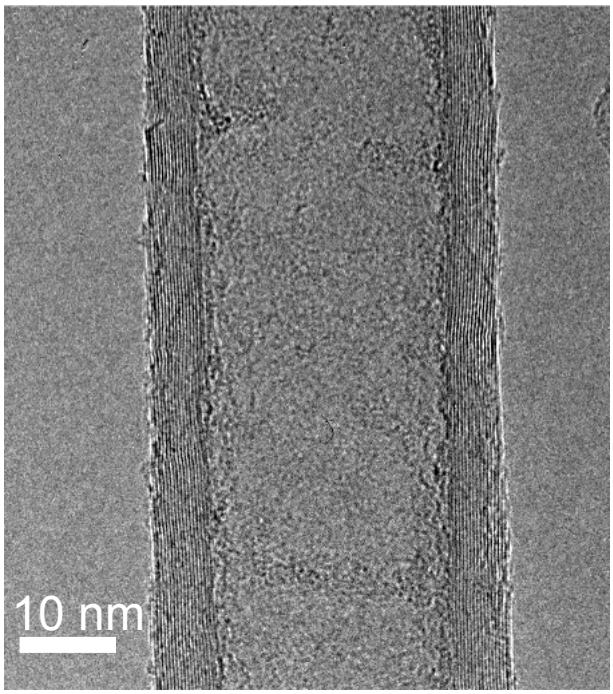

Figure S1: Larger version of the nanotube shown in Figure 1d.

Proportion of Type A and Type B nanotubes within the sample

The morphology of 216 P,N-MWNTs was studied and a table showing the distribution of the different types of morphology is given below. 77% of the nanotubes, were either Type A or Type B. 20% of the nanotubes were very small, and often curled and containing particles. Although 20% in numbers is a lot, the contribution of these small nanotubes towards the properties of the overall ensemble is expected to be negligible due to their small weight percent. Only 3% of the nanotubes (i.e. 7 out of 216 nanotubes) did not fall into one of these three categories

Morphology	**% of sample**
Type A	36
Type B	41
Very small nanotubes	20
Other	3

Transition from a Type A to a Type B nanotube

Figure S2 shows a larger image of the nanotubes shown in Figure 1a which changes from Type A (right-hand side) to Type B (left hand side).

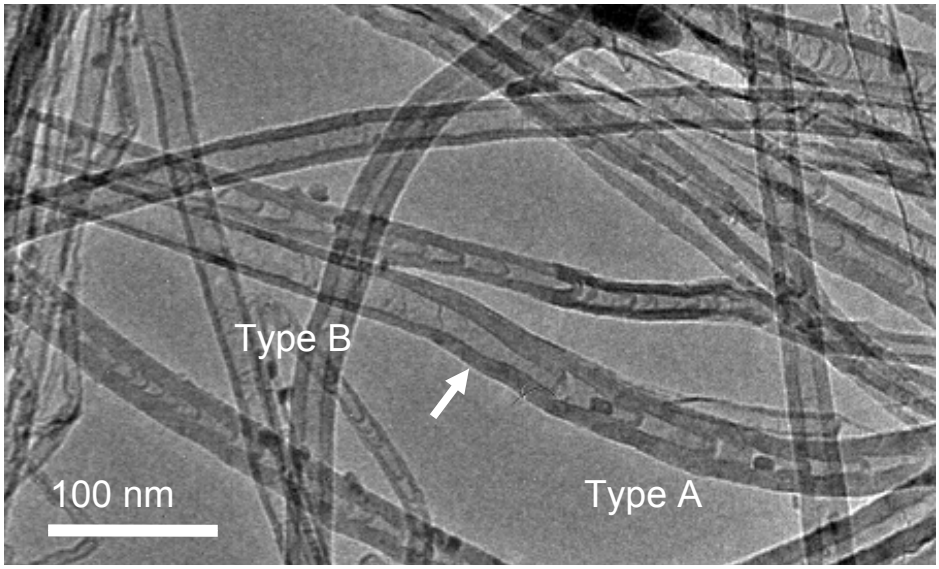

Figure S2: Nanotube (shown in Figure 1a) which changes from Type A (right-hand side) to Type B (left hand side).

Variation in nitrogen content along a nanotube

The nitrogen content was measured at different positions in three Type A and four Type B nanotubes (Figure S3).

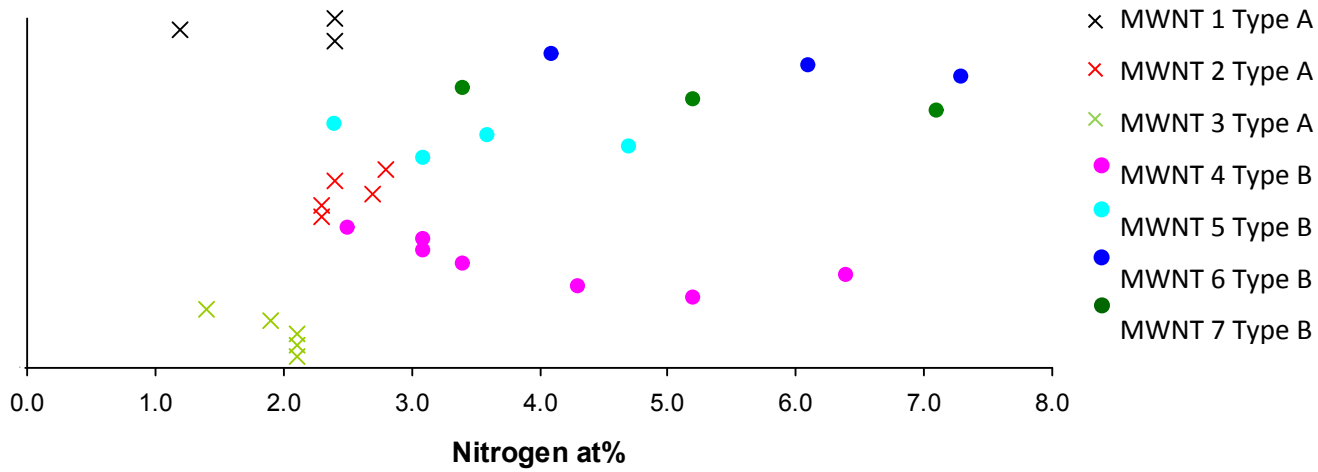

Figure S3: Variation in nitrogen content along seven different nanotubes. Each nanotube is represented by a different colour and each point has been offset by an arbitrary value in the y-direction to make the data easier to interpret.

Presence of N_2 in the inner channel of a Type B P,N-MWCNT

Figure S4a shows the sum of the spectra from pixels 8 – 10 of Figure 3d. The π* peak is very pronounced, indicating the presence of nitrogen gas. It is likely that the spectrum from an entire Type B nanotube (e.g. Figure 3b) contains a signal from bonded nitrogen on or in the walls of the tube as well as from N_2 gas along the central channel. The combination of bonded nitrogen and N_2 gas will reduce the prominence of the π* peak compared with only N_2 gas. The nitrogen signal from pixels 7 and 11 does not show such a strong π* peak and so the total signal from the nanotube (shown in Figure S4b) looks more like that shown in Figure 3b.

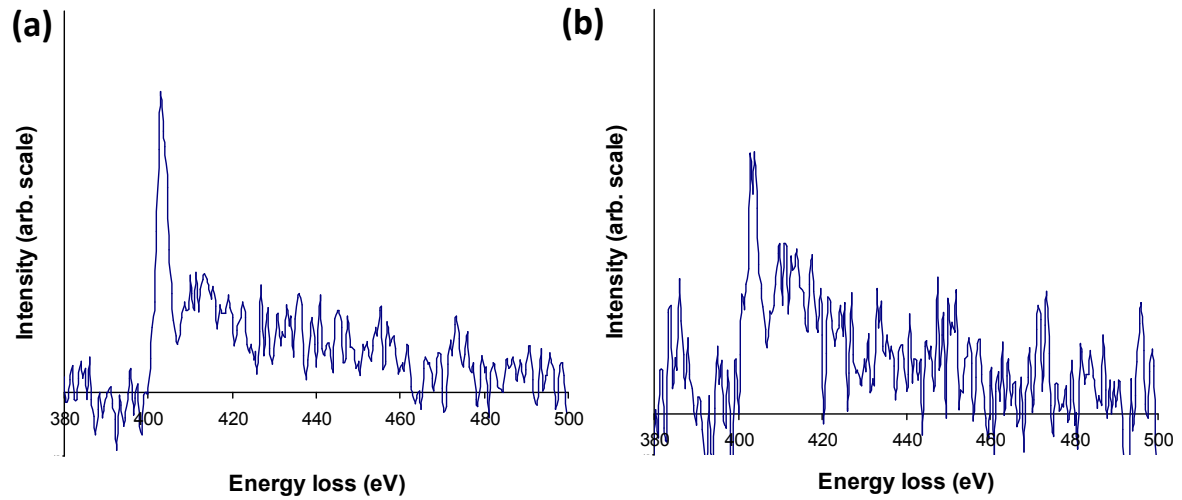

Figure S4: (a) EELS spectra showing the presence of N_2 gas obtained from the centre of a Type B P,N-MWCNT. (b) The total nitrogen EELS signal from the same Type B P,N-MWCNT.

Beam irradiation of a Type B P,N-MWCNT

Figure S5b shows the amorphous structure created by beam irradiation of a Type B nanotube. Nitrogen is still detected within the structure, (Figure S5c).

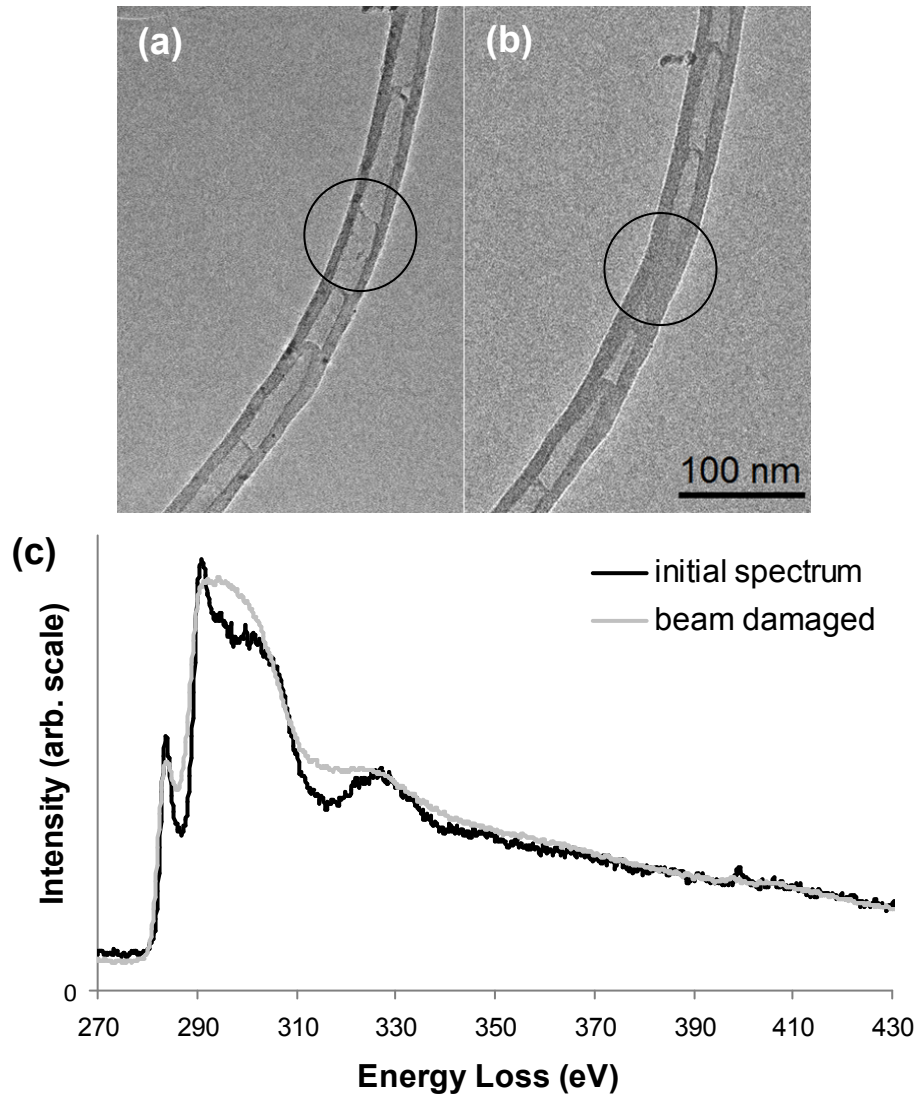

Figure S5: TEM micrographs of a nanotube before (a) and after (b) beam irradiation. The corresponding EELS spectra are shown in (c).

Phosphorus EELS signal from catalyst particle

Figure S6 shows the same catalysis particle as in Figure 4, along with the corresponding phosphorus L-edge EELS signal.

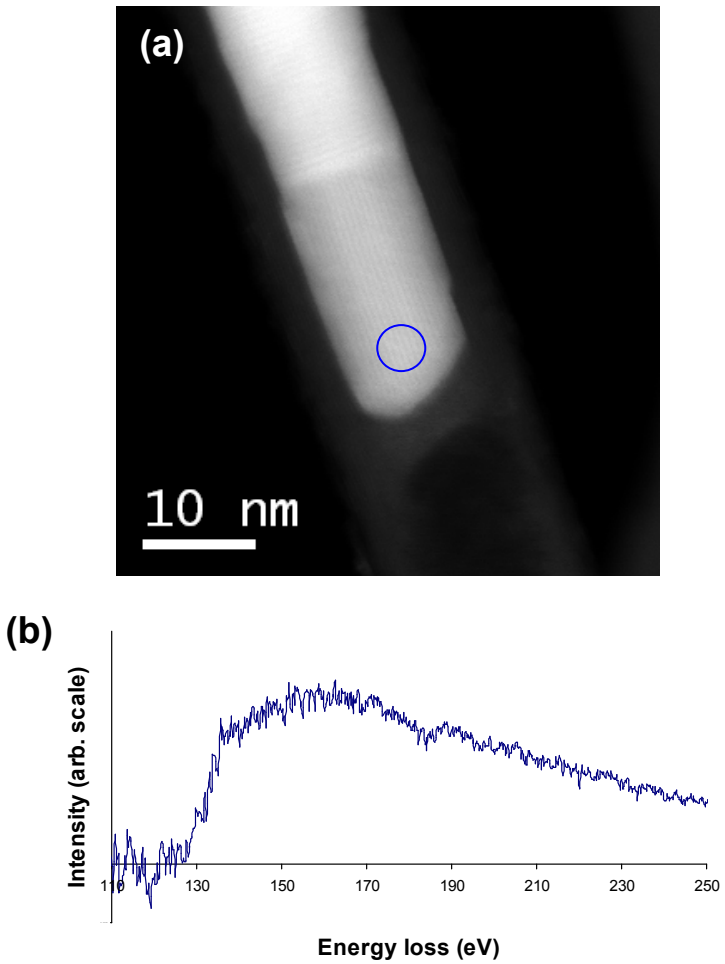

Figure S6: HAADF image (a) and phosphorus L-edge (b) from the region marked in (a).